# Enhanced Integrated Indoor Positioning Algorithm Utilising Wi-Fi Fingerprint Technique

A.S. Ja'afar[1,2], G. Markarian[1], A.A.M. Isa[2], N. A. Ali[2], M.Z.A. Abd Aziz[2]
[1]*School of Computing and Communication*
*Infolab21, Lancaster University, United Kingdom*
[2]*Center for Telecommunication Research & Innovation (CeTRI)*
*Faculty of Electronic & Computer Engineering*
*Universiti Teknikal Malaysia Melaka (UTeM), Malaysia*
*shukur@utem.edu.my, a.jaafar@lancs.ac.uk*

***Abstract*— This paper describes an integrated positioning algorithm utilizing Wi-Fi fingerprint technique for indoor positioning. The main contribution of this work is the improvement of positioning accuracy for indoor localization even in extreme RSSI fluctuation which leads to variation of positioning error. Several layers of Wi-Fi positioning is proposed, which are based on deterministic techniques, iterative Bayesian estimation, and also Kalman filter to enhance accuracy due to noise presence. Here, accumulated accuracy is introduced where the distribution of location error is determined by estimation at each test point on path movement. The results show that the integrated algorithm enhances the estimation accuracy in several scenarios which are different Wi-Fi chipsets and movement directions. The error distribution shows an achievement of up to 65% for error less than 5m compared to the basic deterministic technique of only 45%.**

***Index Terms*– Indoor Positioning; Wi-Fi Fingerprint; Localization.**

## I. Introduction

The growing interest in indoor location-based services (ILBS), due to demands for its application in personal navigation, billing and information enquiries, has expedited the development of research in innovative positioning techniques. The widely used global positioning system (GPS) is a proven technology for outdoor positioning and navigation, but it performs poorly indoor [1][2]. This is due to the fact that the GPS signal cannot penetrate in indoor environment. Other wireless positioning system (WPS) such as wireless broadband communication based on long term evolution (LTE) system only can give best accuracy ranging from 10-15 meters in rural and suburban area [3]. This accuracy cannot be accepted for indoor positioning as 5 meters location error will lead to another section or room in building. Hence, researchers seek alternative solutions, including the concept of signal of opportunity (SoOP) for indoor positioning [4]. The SoOP includes the Wi-Fi, Bluetooth, RFID, magnetic field and FM radio. We concentrate on cheap solutions in mind by utilizing available communication system infrastructure without the need to deploy new transmitters or beacons for positioning purposes. Therefore, the widespread availability of Wi-Fi access points (APs) in building makes it our choice to utilize it as the main indoor positioning.

The main challenge for an indoor positioning system is the non-line of sight (NLOS) condition. The layout and geometry of a building are factors that can put a signal into reflection mode whereby multipath fading could occur and decrease positioning accuracy. Therefore, conventional outdoor localization based on trilateration and triangulation [5], [6] do not work well for indoors with many geometry shape, obstacles and room partitions. In high WLAN coverage, Wi-Fi fingerprint gives promising technique that has better positioning accuracy [7].

In unplanned building conditions where the available number of APs is limited and the locations of APs are predesignated, certain positioning algorithms do not perform well consistently. In addition, there are several other factors that influence positioning accuracy, such as different Wi-Fi chipset manufacturers and different path movements of users. One of the main problems is fluctuation of received signal strength reading from access point to the user [8]. This is more severe to the 2.4GHz operating frequency than 5GHz. Lui et al. [9] have highlighted several problems with different Wi-Fi chipset receivers. The sensitivity of the receiver's chipset built into different devices varies in cost and it is expected that different receiver's chipset at the same location will provide different accuracy of received signal strength indicator (RSSI), hence leading to different accuracy in positioning. Some of the challenges of different Wi-Fi chipsets are that some of them have "dropout of data" in which the RSSI level scanned suddenly falls and recovers. Another phenomenon is the signal strength "catching". This can be described as the RSSI of signal level observed to be stable for a large period of time before it responses to change in reading.

To overcome these challenges, many techniques have been proposed, such as collaborative positioning techniques [10], data fusion of radio-based positioning and mobile-based positioning that uses sensors to sense the physical movement activity of users [11]. Wi-Fi fingerprint acts as the main positioning technique replacing the GPS for indoor environment before fusing with other sensor based localization techniques. If the Wi-Fi fingerprint technique gives a lower accuracy, this will influence the final location estimation. Hence, this is why researchers are still looking for improvement of Wi-Fi fingerprint localization. The first fingerprint technique is based on deterministic technique [12] which is less complex and has low accuracy due to fluctuation of RSSI from APs. The probabilistic method gives more accurate but increases algorithm complexity. One of the techniques to overcome the RSSI level from different devices or device adaptations is on signal strength difference [13] and signal strength ratio [14]. However, manual data collection on each device makes it labor cost intensive and the achievement still suffers from signal noise fluctuation.

In this paper combination layer of localization algorithm is introduced for indoor positioning utilizing Wi-Fi fingerprint technique. The algorithm is based on deterministic technique which is enhanced weighted K-NN (EWKNN) combined with iterative Bayesian estimation for more accurate location estimation. The last layer is filtering layer where Kalman filter is implemented to give final user location estimation. Comparison of the proposed algorithm is made to conventional fingerprint technique in several scenarios like different Wi-Fi chipsets, different path movements and different RSSI samples.

The rest of the paper is structured as follows: Wi-Fi integrated fingerprint technique is outlined in section II; simulation results are highlighted in section III; and conclusion and future work in section IV.

## II. WI-FI INTEGRATED FINGERPRINT TECHNIQUE

The main idea of the algorithm is combination of several layers of process before the final location can be estimated. Figure 1 shows the concept of the proposed indoor localization algorithm. The widespread of WLAN in the building makes it the favorite choice for indoor positioning. The main input parameter will receive the signal strength indicator (RSSI) from Wi-Fi module. The chosen method in this research is Wi-Fi fingerprint technique which involves collection of signals to create the radio map. Later the closest pattern match between the sample vector signal and the radio map will determine the early location of that particular signal. At the early estimation stage, Bayesian estimation was implemented and the accuracy depends on number of RSSI vector sample. Finally, Kalman filter was implemented in filtering layer to improve the location accuracy.

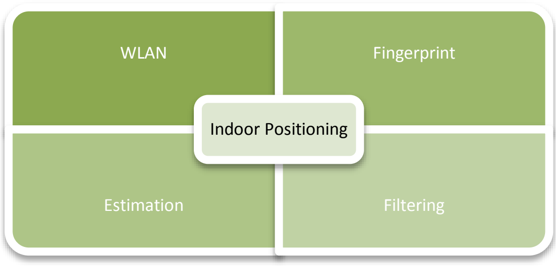


Figure 1: Indoor positioning concept

### A. *Fingerprint technique*

Wi-Fi fingerprint is usually conducted in two phases. The first phase is an offline phase where the vector of RSSI from different access points (APs) at particular reference points (RPs) location are collected. All RSSI vectors and information are stored in a database. The second phase is online phase where the samples of RSSI vector at test point (TP) location are compared to the database. The closest match RSSI vector between online and offline will return the closest estimate location.

Our site survey took place on the B floor Infolab21, School of Computing and Communication, Lancaster University. Figure 2 shows the layout of the building and the site, which consists of a big space in the middle surrounded by lecturers' and researchers' room, and a narrow hallway towards the end of the site. These two different kinds of area zones were purposely selected to study the effectiveness of a single algorithm in various building shapes. Unlike outdoor localisation, 5 m accuracy will have a significant impact in indoor localisation as it can direct the user to an incorrect path or room. This is why improving accuracy is a huge challenge for indoor localisation. The yellow shade on the building layout shows the site survey coverage area while the blue triangle shapes are the available APs location.

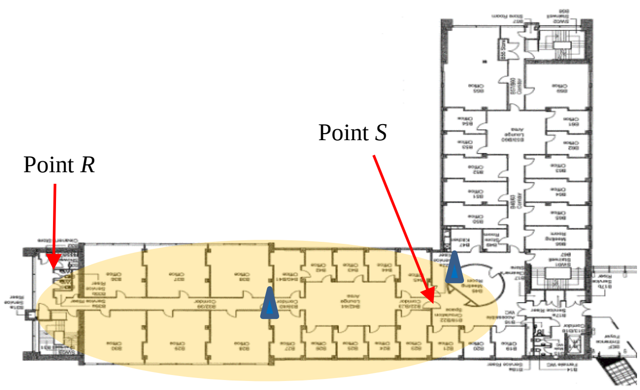


Figure 2: Layout of B floor, Infolab21

There are numerous techniques for position estimation based on collected observations. One common method is K-Nearest Neighbor (K-NN) [15]. K-NN works by "comparing" observation values during an on-line phase and observation of mean values during an off-line phase. To facilitate simple and fast algorithm calculation, a deterministic method was chosen. We decided to implement the Enhanced Weighted-KNN (EWKNN) which has a dynamic selection of K distance [8]. Unlike conventional K-NN which is fixed in terms of distance neighbor point selection, the various space and geometry of the building may reduce the accuracy if constant number of neighbor distance is selected. So, for various geometrical shapes of building, the EWKNN is a more suitable deterministic algorithm. However, the instability of RSSIs (obviously on 2.4GHz) during the on-line phase compared to each mean RSSI's value in the database will return a scattered pattern of estimated positions. If a simple average of estimated positions is taken, the final estimated location will also fluctuate according to the number of RSSI. To overcome this problem, iterative Bayesian estimation was implemented in the algorithm. This technique needs less sampling of RSSI numbers and returns stable position estimations. Each new RSSI value in the on-line phase is compared to the database through the EWK-NN algorithm and an early estimated position will be retained. In this algorithm, 10 RSSIs or more is sufficient to get stable results.

### B. *Estimation*

Unlike other researchers, we implemented dynamic *localization region* instead of clustering techniques. Clustering technique is a method for grouping a set of objects with the same group characteristics to reduce the computational cost by reducing RP searching. In dynamic localization region, the user location history profiling is considered which utilizes Bayesian technique. Dynamic localization region act like mini cluster region however it is in dynamic shape which changes depend on prior location. The Bayes rule can be written as [16]:

$$p(s|x) = \frac{p(X|S) \cdot p(s)}{p(x)} \tag{1}$$

where $s$ is state location, $x$ is observation which in this case is RSSI data, $p(s|x)$ is a posterior estimate of state, and $p(x|s)$ is the likelihood of an observation's given state condition.

$$p(x|s) = \frac{1}{\sigma\sqrt{2\pi}} e^{\left(-(x-s)^2/(2\sigma^2)\right)} \tag{2}$$

Here, $x$ is the observation vector of RSSI and $s$ is the RPs location in localization region. For a higher dimensional condition, we use multivariate Gaussian distribution as the location in this situation is in two dimensions and consists of planes X and Y. Then, the density function of multivariate Gaussian distribution is given by:

$$p(x_1, \ldots, x_k|s) = \frac{e^{\left(-\frac{1}{2}(x-s)^T \Sigma^{-1}(x-s)\right)}}{\sqrt{(2\pi)^k|\Sigma|}} \tag{3}$$

where $x$ is a k-dimensional column vector, $\sum$ is a covariance matrix, and $|\Sigma|$ is the determinant of the covariance matrix.

In the implementation of Bayes rules, information about prior position is as important as the object movement history. From a prior position, the next possible user location is estimated within certain area coverage. This coverage area comprises several adjacent RPs' locations surrounding the prior location, which might be a possible actual location during localization. We call this coverage area the *localization region*, where the next possible actual location will be in this area. In this case, assumption has been made that the user movement is less than the size of the adjacent RPs which is 1.5m over 1s. Based on prior location, we can determine all adjacent RP locations which are listed in a lookup table. Different prior locations will give different lists and total numbers of adjacent RP locations due to the different geometries of buildings. Figure 3 depicts the localization region where a localization process will determine an estimated location in this region. In this figure, a user is shown to be walking from left to right in sight of the building through a hallway and an open square space. The localization region can be dynamic in shape depending on prior location and building geometry. In addition, the localization region will be updated in each cycle of the localisation process.

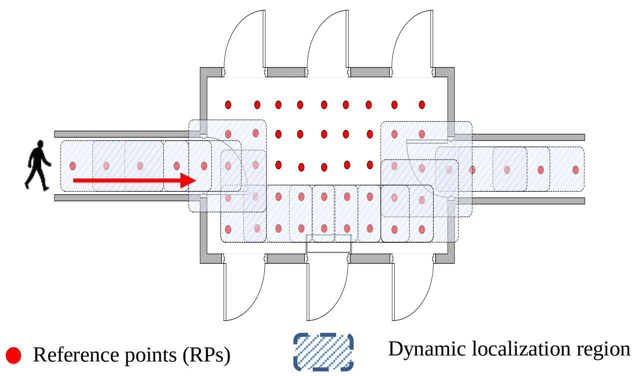


Figure 3: Dynamic localization region

The likelihood function needs to be calculated for each early position from EWK-NN to give each possible RP location in the *localization region*. The return value of the likelihood function is retained and used in the next iterative cycle process until there are enough RSSI values for each location. After completing the iterative process, the position is estimated from the highest return probability value based on the possible RP location points. The new position estimated will become the new prior position for the next iterative process and the lookup table for RPs adjacent to the current position will be updated. This cycle will be repeated in the next localization process.

### *C. Kalman Filter*

To smoothen the presence of noise, Kalman filter was implemented in the last layer [17]. The Kalman filter has been extensively used in estimating the state condition of a process [18][19]. The state of a moving object is represented as $X$ in the process, where vector $X$ consists of a moving object's $x$ and $y$ coordinates and its velocity. The system that is considered is as follows:

State model: $X_k = AX_{k-1} + W$ (4)
Measurement model: $Z_k = HX_k + V$ (5)

$$\hat{X}_k = \begin{bmatrix} x_k \\ y_k \\ v_{xk} \\ v_{yk} \end{bmatrix}, \quad A = \begin{bmatrix} 1 & 0 & \Delta_t & 0 \\ 0 & 1 & 0 & \Delta_t \\ 0 & 0 & 1 & 0 \\ 0 & 0 & 0 & 1 \end{bmatrix},$$

$$H = \begin{bmatrix} 1 & 0 & 0 & 0 \\ 0 & 1 & 0 & 0 \end{bmatrix}, \quad Z_k = \begin{bmatrix} x_k \\ y_k \end{bmatrix}$$

Then the remaining steps of Kalman filter repeats evaluating expressions 6-9 including the prediction of state and error covariance, Kalman gain, estimation process, and updates the error covariance.

$$P_k^- = AP_{k-1}A^T + Q \tag{6}$$

$$K_k = P_k^- H^T (HP_k^- H^T + R)^{-1} \tag{7}$$

$$\hat{x}_k = \hat{x}_k^- + K_k(z_k - H\hat{x}_k^-) \tag{8}$$

$$P_k = P_k^- - K_k H P_k^- \tag{9}$$

The processes start with initializing the $\hat{x}_k$ and $P_0$ from expression 4 and 5. On the Kalman filter estimation process, the input will be from measurements which come from early location estimation process and the output will be the final location estimation. Q and R are the process noise covariance matrix and measurement noise covariance matrix. These two parameters will affect the measurement and prediction of the Kalman filter process. Between these parameters, process noise covariance is hard to determine. These are determined by experience or experiment. Yim et al. in [17], [20] have highlighted based on his experiment the ratio between Q and R that really affects the performance of the Kalman filter. By following the same step, based on our measurement data, it was found that Q equal to 0.00001 gives optimum results. The initial condition setup is as follows:

$$Q = \begin{bmatrix} 0.00001 & 0 & 0 & 0 \\ 0 & 0.00001 & 0 & 0 \\ 0 & 0 & 0.00001 & 0 \\ 0 & 0 & 0 & 0.00001 \end{bmatrix}$$

$$R = \begin{bmatrix} 1 & 0 \\ 0 & 1 \end{bmatrix}$$

$$P_0 = \begin{bmatrix} 5 & 0 & 0 & 0 \\ 0 & 5 & 0 & 0 \\ 0 & 0 & 5 & 0 \\ 0 & 0 & 0 & 5 \end{bmatrix}$$

$$\hat{x}_k = \begin{bmatrix} 32.75 \\ 2.75 \\ 0 \\ 0 \end{bmatrix}$$

## III. SIMULATION RESULTS AND ANALYSIS

To evaluate the accuracy of user location, we calculated the term "accumulated accuracy" to get early assumption from distribution error of location graph. Accumulated accuracy is given by:

$$A = \int_0^n \sqrt{\left(f(n) - f_o(n)\right)^2}\, dn \qquad (10)$$

where $f(n)$ is the relative positioning graph under TPs
$f_o(n)$ is the base line of zero error

We analyzed our hypotheses based on several factors that influence the positioning accuracy. These factors are:

- Movement direction: The direction of path movement chosen is from point S to point R and vice versa.
- Different Wi-Fi chipset: Two different devices were used during the online phase. The first mobile device uses a Qualcomm Atheros chipset which is the same Wi-Fi chipset used during the site survey, while the second device used is a Broadcom Wi-Fi chipset. The results from the two different chipsets used were then compared.
- Number of RSSIs samples before estimation: As mentioned in previous section, at least 10 RSSI samples are needed to get accurate and stable localization. Here, different numbers of RSSI samples were included in our algorithm. The samples start with 25 RSSI and then doubled to 50 RSSI signal samples.

### *A. Movement Direction from Point R to Point S*

In this scenario, the performances of several algorithms on different movement directions and different Wi-Fi chipsets were investigated. The layout site was on B floor, Infolab21, School of Computing and Communication, as shown in Figure 2. Based on the layout, there are two paths with different directions. In the first condition, the user moves from point R to point S, while in the second condition the user moves from point S to point R. The last factor mentioned is different Wi-Fi chipsets. In this scenario, two types of well-known chipsets were used, i.e. the Quantum Atheros and Broadcom chipsets.

Our simulation started with movement direction from point R to point S. During the on-line phase, RSSIs were sampled at each dedicated TP location for each direction. The error distribution for each TP location is presented with different types of algorithms included in our proposed algorithm. Figure 4 shows the distribution of errors for our proposed algorithm (EWKNN+Bayes+Kalman filter) compared to other positioning algorithms for movement direction R to point S, for a Qualcomm Atheros Wi-Fi chipset with 25 sample RSSIs. All the error location is mapped to the TPs location itself. One of the reasons is to identify the region of higher location error due to non-line of sight condition of building geometry. This information is needed in next chapter in this research. Based on the graph, it is clear that only the proposed algorithm gives constant error distribution of below 5 meters, which are EWKNN with Bayesian estimation and a Kalman filter. With the deterministic algorithm K-NN and WKNN, location error rises suddenly at more than 20 meters from TP points 6 to 10. It is clear that a combination of uncertain RSSI values from APs causes the location error distribution to fluctuate. Our algorithm, which works based on a localization region, performed well to contain errors in this kind of situation but with a short period of huge localization errors from point 6 to point 10.

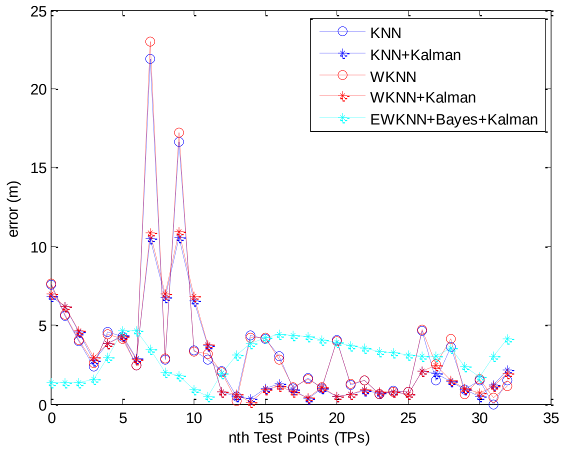


Figure 4: Error distribution for a Qualcomm Atheros Wi-Fi chipset with 25 RSSI samples.

In addition, error distributions were plotted using the same algorithm based on 25 RSSI samples using a Broadcom Wi-Fi chipset. The results in Figure 5 show different error distribution pattern compared to that of Figure 4. This clearly shows that different Wi-Fi chipsets have different readings of RSSI value due to different levels of sensitivity hence returning different levels of positioning accuracy. Based on the graph, a conventional K-NN and WKNN algorithm shows that positioning errors start to hit 5 meters from TP points 21 to 29. In this scenario, the gradually increasing errors are the main reason that the proposed algorithm - EWKNN+Bayes+Kalman filter algorithms follows the same pattern. This is because in a conventional deterministic algorithm, there is increasing location error from TP point 21 onwards, where the localization region calculated keeps the process in the wrong region. Therefore, positioning error also increases gradually like the conventional deterministic algorithm.

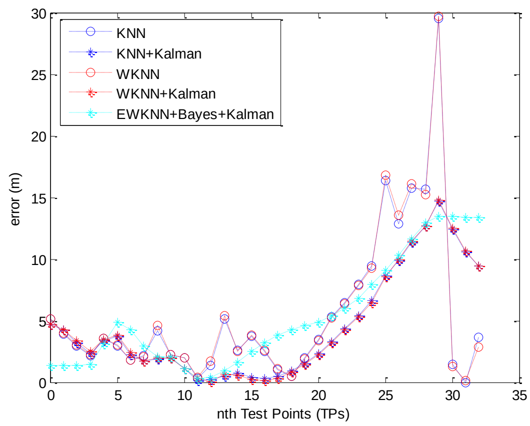


Figure 5: Error distribution for a Broadcom Wi-Fi chipset with 25 RSSI samples.

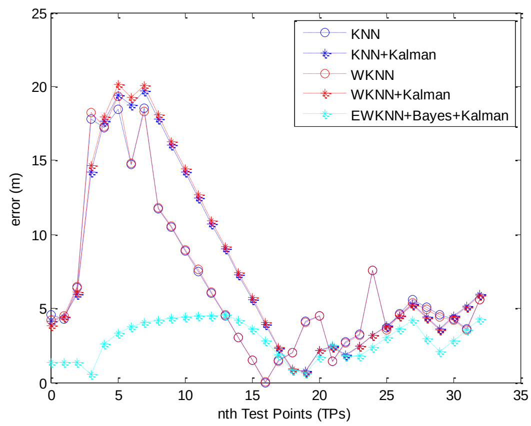


Figure 7: Error distribution for Broadcom Wi-Fi chipset with 25 RSSI samples.

*B. Movement Direction from Point S to Point R*

The error distribution patterns at the same TP locations were then simulated but with movement in the opposite direction. From Figure 6 below, it can be seen that the patterns of error distribution are obviously different, even when using the same Wi-Fi chipset (Qualcomm Atheros) and number of RSSI samples. This is because when movement direction is in the opposite direction, the blockage and reflected signals do not follow the same path as before. The user's body and antenna radiation pattern could give readings of signal strength at different levels, thus giving different positioning accuracy, even at the same location. In this scenario, our proposed algorithm performed well below 5 meters, until it reached TP point 18. However, from this point onwards, the overall distribution is still slightly better than the basic deterministic techniques.

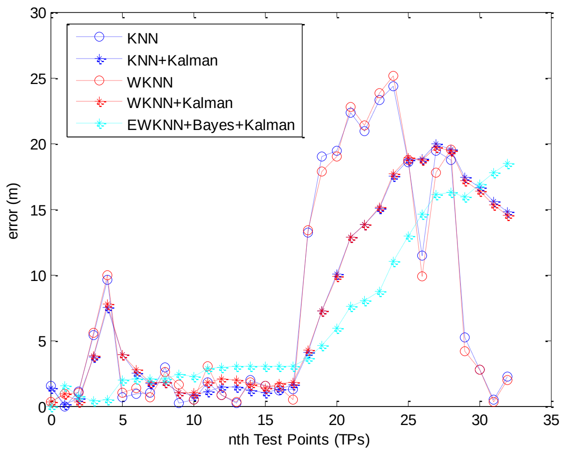


Figure 6: Error distribution for Qualcomm Atheros Wi-Fi chipset with 25 RSSI samples.

In the same direction, the RSSI data collection then changed to Broadcom Wi-Fi chipset. The proposed algorithm performs very well along the path from point S to point R, as depicted in Figure 7. The location error is consistently below 5 meters for all TP locations compared to the basic deterministic techniques showing heavy fluctuation in positioning.

Then, the overall simulation was repeated with doubled number of RSSI samples. The results show that the pattern of error distribution is almost similar as shown in Figure 4 to Figure 7. The accumulated accuracy then is recorded in Table 1 displayed in the next section.

*C. Overall Results*

The accumulated accuracy of eight combinations with different kinds of parameters, such as Wi-Fi chipsets, movement direction and the number of RSSI samples are presented in Table 1. As can been seen, the effects of the number of RSSI samples for all the scenarios are almost insignificant. The accumulated accuracy in Table 1 shows that across all algorithms for both 25 and 50 RSSI samples, the numbers are not very different. This shows that even increasing the number of RSSI samples does not significantly improve positioning accuracy. In some cases, positioning accuracy results are better with fewer RSSI samples. In three out of four different scenarios, the accumulated accuracy shows that the proposed algorithm is better than the basic deterministic technique (K-NN and WK-NN) and deterministic with Kalman filter.

Table 1
Accumulated accuracy based of different algorithms.

| Direction | Wi-Fi Chipset | Number of RSSIs samples | Algorithms | | | | |
|---|---|---|---|---|---|---|---|
| | | | K-NN | WKNN | K-NN +Kalman Filter | WKNN + Kalman Filter | EWKNN + Bayesian + Kalman Filter |
| Point R to Point S | Qualcomm Atheros | 25 | 118.528 | 121.7752 | 101.7806 | 103.4829 | 92.7658 |
| | | 50 | 125.6128 | 128.8719 | 106.3673 | 107.8658 | 94.2072 |
| | Broadcom | 25 | 179.7866 | 181.2023 | 147.4695 | 147.2358 | 176.1536 |

| Point S to Point R | | | | | |
|---|---|---|---|---|---|
| Broadcom | | Qualcomm Atheros | | | |
| 50 | 25 | 50 | 25 | 50 | |
| 223.9111 | 219.5944 | 260.3334 | 254.0451 | 176.8632 | |
| 225.4635 | 220.535 | 259.4693 | 253.2184 | 177.4372 | |
| 264.5392 | 254.8172 | 256.0950 | 255.9532 | 149.6832 | |
| 268.6933 | 257.7336 | 258.0509 | 258.6883 | 148.2570 | |
| 94.1010 | 95.8129 | 226.8049 | 215.4907 | 161.4242 | |

Based on all scenarios in Table 1, the results were plotted in terms of cumulative distribution function (CDF) vs location error (m) as depicted in Figure 8. The basic K-NN and WKNN algorithm both give 45% of error less than 5 meters. Improvement of current algorithm with Kalman filter did improve another 4% to ~49% of confident location error of less than 5 meters. However, our proposed algorithm (EWKNN+Bayesian estimation+Kalman filter) improves by 20% compared to basic deterministic algorithm. The CDF graph shows up to ~65% for location error of less than 5 meters, and almost 100% confident in error of less than 10 meters.

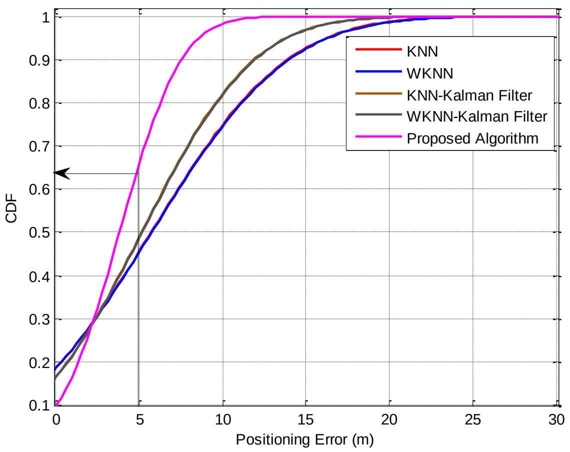


Figure 8: CDF of location errors

## IV. CONCLUSION AND FUTURE WORK

In this paper, we have described the combination of several layers of localization algorithm to enhance indoor positioning accuracy. Several combination scenarios including different kinds of Wi-Fi chipset, different movement paths and different samples of RSSI have been investigated. The results show that increasing number of RSSI samples by double does not significantly improve the location accuracy. The proposed algorithm shows that the estimation error are in better control for both different Wi-Fi chipset and path movement compared to the conventional deterministic techniques. The CDF of the proposed algorithm gives 65% accuracy for error less than 5 meters while both conventional K-NN and WK-NN just 45%. These show the accuracy improvement of 20%. To further enhance the overall accumulated accuracy along the path movement, the proposed algorithm can be suitable to get the calibration point in order to prevent accumulated error from occurring. In the future, further investigation needs to be done on position of suitable calibration point with the proposed indoor location algorithm. The distribution location error graphs in this research are the key to calibration point in the next research.

## ACKNOWLEDGEMENT

The authors appreciate Universiti Teknikal Malaysia Melaka (UTeM) and Ministry of Education Malaysia for their sponsor and support.

## REFERENCES

[1] P. D. Groves, *Principle of GNSS, Inertial, and Multisensor Integrated Navigation Systems*. ARTECH HOUSE INC, 2008.

[2] P. D. Groves, L. Wang, D. Walter, H. Martin, K. Voutsis, and Z. Jiang, "The four key challenges of advanced multisensor navigation and positioning," *2014 IEEE/ION Position, Locat. Navig. Symp. - PLANS 2014*, no. May, pp. 773–792, May 2014.

[3] M. F. M. Mahyuddin, A. A. M. Isa, M. S. I. M. Zin, A. M. A. H, Z. Manap, and M. K. Ismail, "Overview of Positioning Techniques for LTE Technology," *J. Telecommun. Electron. Comput. Eng.*, vol. 9, no.2, 2017.

[4] V. Moghtadaiee, S. Lim, and A. G. Dempster, "System-Level Considerations for Signal-of-Opportunity Positioning," *Int. Symp. GPS/GNSS*, pp. 1–7, 2010.

[5] Z. Manap, A. A. M. Isa, M. H. Othman, and A. M. Darsono, "Performance Analysis of TOA-based Positioning in LTE by utilizing MIMO Feature," *J. Telecommun. Electron. Comput. Eng.*, vol. 9, no. 2, pp. 117–121, 2017.

[6] H. Liu and H. Darabi, "Survey of wireless indoor positioning techniques and systems," *IEEE Trans. Syst. Man, Cybernertics*, vol. 37, no. 6, pp. 1067–1080, 2007.

[7] S. He, S. Member, S. G. Chan, and S. Member, "Wi-Fi Fingerprint-Based Indoor Positioning : Recent Advances and Comparisons," vol. 18, no. 1, pp. 466–490, 2016.

[8] B. S. -, J. H. L. -, T. L. -, and H. S. K. -, "Enhanced Weighted K-Nearest Neighbor Algorithm for Indoor Wi-Fi Positioning Systems," *Int. J. Networked Comput. Adv. Inf. Manag.*, vol. 2, pp. 15–21, 2012.

[9] G. Lui, T. Gallagher, B. Li, A. G. Dempster, and C. Rizos, "Differences in RSSI readings made by different Wi-Fi chipsets: A limitation of WLAN localization," in *2011 International Conference on Localization and GNSS, ICL-GNSS 2011*, 2011, pp. 53–57.

[10] D. Rodionov, D. Kolev, and K. Bushminkin, "Hybrid Positioning Technique for Indoor Environment," in *1st Annual International Conference on Health &Medical Sciences*, 2013.

[11] J. Cheng, L. Yang, Y. Li, and W. Zhang, "Seamless outdoor/indoor navigation with WIFI/GPS aided low cost Inertial Navigation System," *Phys. Commun.*, Jan. 2014.

[12] P. Bahl and V. N. Padmanabhan, "RADAR: an in-building RF-based user location and tracking system," in *Proceedings IEEE INFOCOM 2000. Conference on Computer Communications. Nineteenth Annual Joint Conference of the IEEE Computer and Communications Societies (Cat. No.00CH37064)*, 2000, vol. 2, no. c.

[13] A. K. M. Mahtab Hossain, Y. Jin, W. S. Soh, and H. N. Van, "SSD:A robust RF location fingerprint addressing mobile devices' heterogeneity," *IEEE Trans. Mob. Comput.*, vol. 12, no. 1, pp. 65 77, 2013.

[14] S. H. Fang, C. H. Wang, S. M. Chiou, and P. Lin, "Calibration-free approaches for robust Wi-Fi positioning against device diversity: A performance comparison," *IEEE Veh. Technol. Conf.*, 2012.

[15] H. Lin, Y. Zhang, M. Griss, and I. Landa, "Enhanced Indoor Locationing in a Congested Wi-Fi Environment," in *MRC-TR-2009*, 2009, no. March, pp. 1–16.

[16] J. H. Anton, *Bayesian Estimation and Tracking: A Practical Guide*. John Wiley & Sons, Inc. Publication, 2012.

[17] J. Yim, J. Kim, G. Lee, and K. Shim, "Kalman filter vs. particle filter in improving K-NN indoor positioning," in *Lecture Notes in*

*Computer Science (including subseries Lecture Notes in Artificial Intelligence and Lecture Notes in Bioinformatics)*, vol. 6882 LNAI, no. PART 2, 2011, pp. 203–213.

[18] R. Faragher, "Understanding the basis of the kalman filter via a simple and intuitive derivation [lecture notes]," *IEEE Signal Process. Mag.*, vol. 29, no. 5, pp. 128–132, 2012.

[19] P. Kim, *Kalman Filter for Beginners, with MATLAB Examples*. A JIN Publishing, 2011.

[20] J. Yim, C. Park, J. Joo, and S. Jeong, "Extended Kalman Filter for wireless LAN based indoor positioning," *Decis. Support Syst.*, vol. 45, pp. 960–971, 2008.